Paper:

Scenarios of Earthquake and Tsunami Damage Probability in Callao Region, Peru Using Tsunami Fragility Functions

Bruno Adriano[*1], **Erick Mas**[*2], **Shunichi Koshimura**[*2], **Miguel Estrada**[*3], and **Cesar Jimenez**[*4,*5]

[*1]Graduate School of Engineering, Tohoku University
Aoba 468-1-E301, Aramaki, Aoba-ku, Sendai 980-0845, Japan
E-mail: adriano@geoinfo.civil.tohoku.ac.jp
[*2]International Research Institute of Disaster Science (IRIDeS), Tohoku University, Japan
[*3]Japan-Peru Center for Earthquake Engineering and Disaster Mitigation (CISMID),
National University of Engineering, Lima, Perú
[*4]Dirección de Hidrografía y Navegación, DHN, Callao, Perú
[*5]Fenlab, Universidad Nacional Mayor de San Marcos (UNMSM), Lima, Perú
[Received July 1, 2014; accepted September 6, 2014]

The implementation of adequate urban development and measures systems against tsunami impact in coastal communities is improved by understanding damage probability among building structures. Within the framework of the project Enhancement of Earthquake and Tsunami Disaster Mitigation Technology in Peru (JST-JICA SATREPS), the authors analyze the damage probability of building structures due to tsunami impact in the Callao region of Peru. Two different tsunami hazard scenarios are assumed in assessing building damage probability. The first tsunami scenario represents the worse-case scenario of tsunami inundation that calculates the envelop of maximum inundation depth and flow velocity values from 12 probabilistic megathrust earthquake scenarios for central Peru. The second tsunami scenario corresponds to a historical tsunami event in this region. We apply a methodology for evaluating different levels of building damage by combining tsunami numerical results and tsunami fragility functions. Damage probability was analyzed in detail on a single building scale in the La Punta district. For the rest of Callao region, analysis was performed on a block-unit scale. Our results suggest that approximately 30% of submerged building may be washed away by tsunami inundation in the probabilistic hazard scenario and approximately 60% in the historical hazard scenario.

Keywords: damage probability assessment, tsunami fragility function, tsunami inundation scenarios in central Peru.

1. Introduction

In Peru's modern seismic history, the three largest, most recent earthquakes of considerable magnitude occurred in the central coastal region of Peru in 1966 (M_w8.1), 1970 (M_w7.9), and 1974 (M_w8.1). Based on the literature [1, 2], these events significantly structurally damaged coastal infrastructures and took human lives. An even more gigantic event, however, considered one of the most catastrophic earthquakes and tsunamis disaster in Peru's history, occurred in 1746 (M_w8.6-M_w8.8) off the central coast [3, 4]. The study presented in [5] reported that ground shaking and subsequent tsunami inundation completely destroyed Callao port. In short, it has been over 250 years since the last megaearthquake and 40 years since the last significant seismic activity in this area. It is thus clear that there has been an absence of earthquakes and tsunamis of large or considerable magnitude in the surroundings of the central Peru coast. Given the seismic history of Callao region in Central Peru, it thus important to take into account the high possibility of the occurrence of a catastrophic seismic event accompanied by an enormous tsunami.

The evaluation of building damages from tsunami impact is used as a starting point for an effective tsunami risk-reduction program [7]. Understanding damage probability among structures in vulnerable coastal areas may improve the implementation of measure against tsunamis and tsunami hazard planning. The authors estimate the damage probability levels to buildings in the Callao region of central Peru. We conduct our analysis based on two hazard scenarios. The first represents the worse-case scenario for tsunami inundation that calculates the envelop of maximum inundation values from 12 probabilistic megathrust earthquake scenarios [8–10]. The second scenario corresponds to the estimated source of the 1746 historical tsunami event [3]. To evaluate different building damage levels, we introduce a novel methodology by combining tsunami numerical results and empirical tsunami fragility functions.
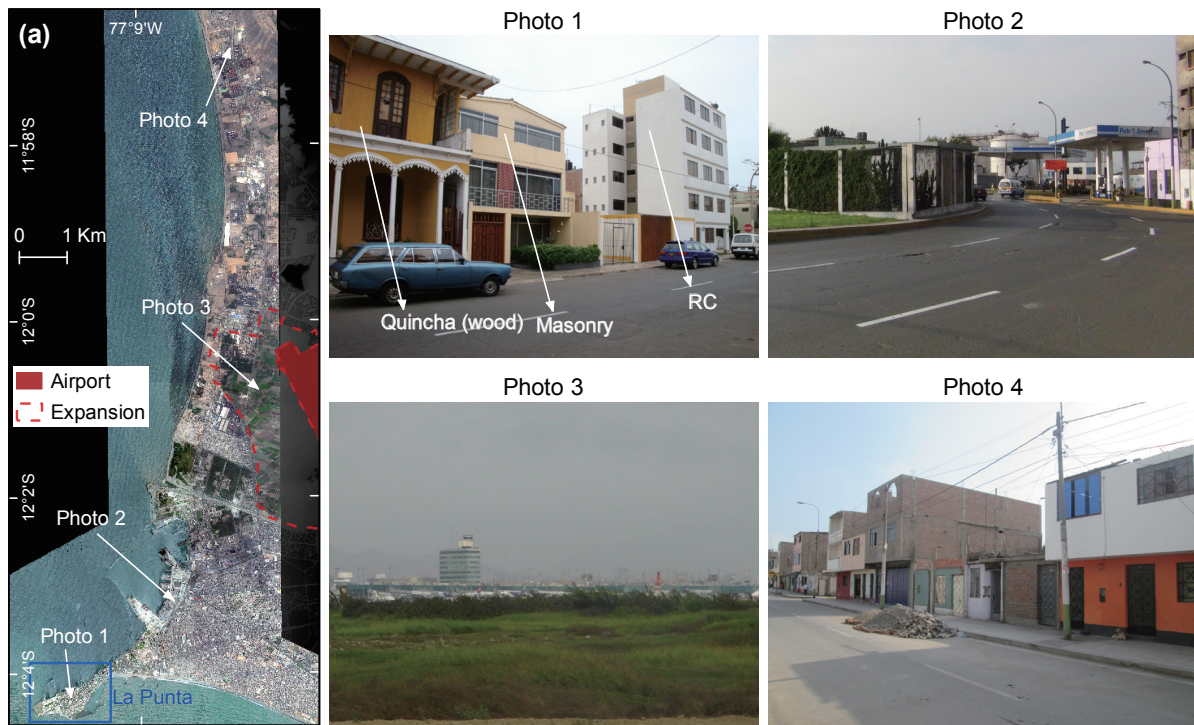
Fig. 1. (a) View of the study area. The red solid-polygon shows part of the area corresponding to the runway of the International Airport Jorge Chavez. The red dashed line shows the projected development of airport facilities [6]. Photos 1-4 show major urban features in the study area. Approximate photo locations are shown in (a).

2. Description of the Study Area

This study covers the central Peruvian coast corresponding to the Callao region (**Fig. 1(a)**). Based on land use, the study area is classified into three main sectors.

The first is located in the southern part of the study area below $12°02'30''$ and corresponds to built-up urban areas. This area is thus the most densely populated area in Callao region (Photos 1-2 in **Fig. 1**). The La Punta district, an small peninsula, is also located in this sector (**Fig. 1(a)**).

The second land use sector is between $12°01'00''$ and $12°02'30''$ and is mainly covered by agricultural fields (Photo 3 in **Fig. 1**). Part of the International Airport Jorge Chavez runway is located inside this sector, as shown by the red solid polygon in **Fig. 1(a)**. Note that a large area in this sector is reserved for future expansion of airport facilities [6], as shown by the red dashed line in **Fig. 1(a)**. There are also several urban communities placed along the coastline.

The third sector is in the northern part of the study area and is mainly occupied by large factories and, to the north, by urban communities (Photo 4 in **Fig. 1**).

2.1. Building Dataset

This study uses two building dataset. A building-unit scale dataset used for the La Punta district contains contains information on the construction material type and number of stories. A block-unit scale dataset constructed by the Peruvian Institute of Statistic and Informatics (INEI) [11] is used for the rest of the study area. Each block-unit has information on the total number of buildings classified by construction material. In this study, both dataset are integrated to form a uniform data file. Based on the construction material, the INEI classified building into six groups for the material used in building walls (**Table 1**). Photo 1 in **Fig. 1** shows an example of three types of buildings, i.e., quincha wood, masonry, and reinforced concrete (RC). The distribution of building type throughout the study area is shown in **Fig. 2**, where it is to be noted that most residential houses in the study area are constructed of brick masonry. Buildings are reclassified into three main groups as follows:

- Masonry: This type of construction uses brick walls confined by vertical RC tie columns. Brick masonry buildings are typically one or two stories (Photo 4 in **Fig. 1**). Adobe masonry structures made from sun-dried bricks are included in this group.

- Wood: This construction uses wood. A similar material, called Quincha, consist of wood put together with cane as a frame covered in mud. These are traditional and older structures in the area, most being part of the cultural heritage. An example of this housing type is shown in Photo 1 in **Fig. 1**.

- RC: This group basically uses RC wall or a RC frame (column bean) as main structural component.

- Others: This group includes structures built using only steel frames or combined with RC. Large factories and warehouses in the north part of the study area predominate in this group.

Table 1. Classification of construction material based on the INEI [11] and equivalent classification used in this study.

INEI's classification	Material (in this study)
Brick	Masonry
Adobe	
Wood	Wood
Quincha	
RC	RC
Others	Others
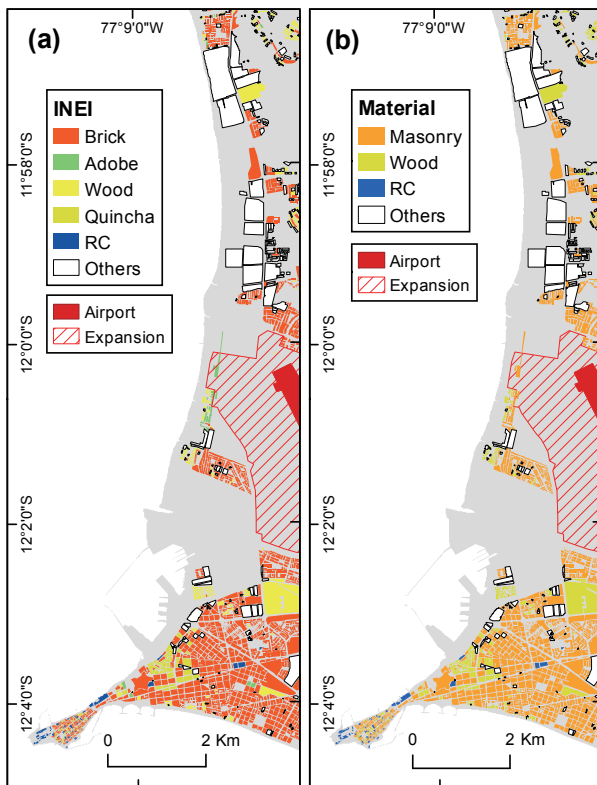
Fig. 2. Building classification in the study area based on construction material. (a) Material distribution based on the INEI [11]. (b) Equivalent classification used in this study.

3. Tsunami Hazard Scenarios

Hazard scenarios used to assess damage probability in Callao region are defined below. In previous studies, tsunami hazards were presented represented by a set of inundation maps mainly calculated through numerical calculations assuming a historical seismic event in the region of interest as an earthquake source [12–16]. In the case of Peru, previous studies evaluating tsunami vulnerability in the study area have used either empirical equations or numerical calculations to estimate tsunami hazards in terms of maximum tsunami height [17, 18]. Most recently, within the framework of the Japan-Peru JICA-SATREPS project, a more realistic tsunami hazard has been introduced for the central region of the Peru coast [19]. Adriano et. al [19] estimated a set of detailed inundation maps, and evaluated potential human casualties due to tsunami

flooding [20, 21]. To evaluate the probability of building damage, we define two different tsunami hazard scenarios in this study in terms of maximum tsunami inundation depth and flow velocity. The first tsunami hazard (Case 1) scenario represents the worse-case scenario of tsunami impact that calculates the envelop of maximum tsunami inundation depth and flow velocity from 12 probabilistic megathrust earthquake sources in central Peru [8–10]. The second tsunami hazard (Case 2) scenario corresponds to numerical results for a historical tsunami event considered to have been one of the most catastrophic seismic events in Peru's history [3]. The tsunami hazard scenarios are shown in **Fig. 3**.

Figure 3 shows the significant difference between hazard scenarios, which is clearly observed by comparing the inundation area in both cases (**Figs. 3(a)-(b)**). In the case of inundation depth, Case 1 has areas approximately 8 m inundation depth that are mostly concentrated in the northern sector of the study area, and areas up to 6 m inundation depth in the southern sector where most urban areas are largely located.

Conversely, Case 2 inundation depth values are almost twice the height of those in Case 1. Case 2 has 16 m depth in the northern sector and 12 m depth in the southern sector.

Regarding tsunami flow velocity, both case scenarios reach values approximately over 9 m/s. It is also clear, however, that Case 2 presents more areas where flow velocity is higher than Case 1 presents (**Figs. 3(c)-(d)**). These areas are mostly concentrated in the center of the study area and are mainly covered by agricultural fields. An important fact in both scenarios is that the tsunami flood reaches part of the area destined for future expansion of the International Airport Jorge Chavez [6]. The flooded area in Case 2 also extents to part of the actual runway zone of the international airport (**Figs. 3(b)** and **(d)**).

4. Tsunami Vulnerability Assessment

The 2011 Tohoku tsunami disaster demonstrated the destructive power of tsunami inundation features in coastal infrastructures [22–25]. Recent studies have demonstrated that damage to coastal structures follows a dynamic component that depends on a number of parameters. The Papathoma Tsunami Vulnerability Assessment (PTVA) model, for example, was developed to assess building vulnerability to tsunami impact, and considers the coastal setting for identifying and ranking a series of attributes such as building use, construction material, and spatial location, for estimating tsunami damage to buildings [12, 26, 27]. In another approach, the work presented in [28], which uses a large database of building damage from the 2011 Japan tsunami, identifies a set of variables, i.e., inundation depth, structural material, and building function, that may be correlated with the level of building damage.
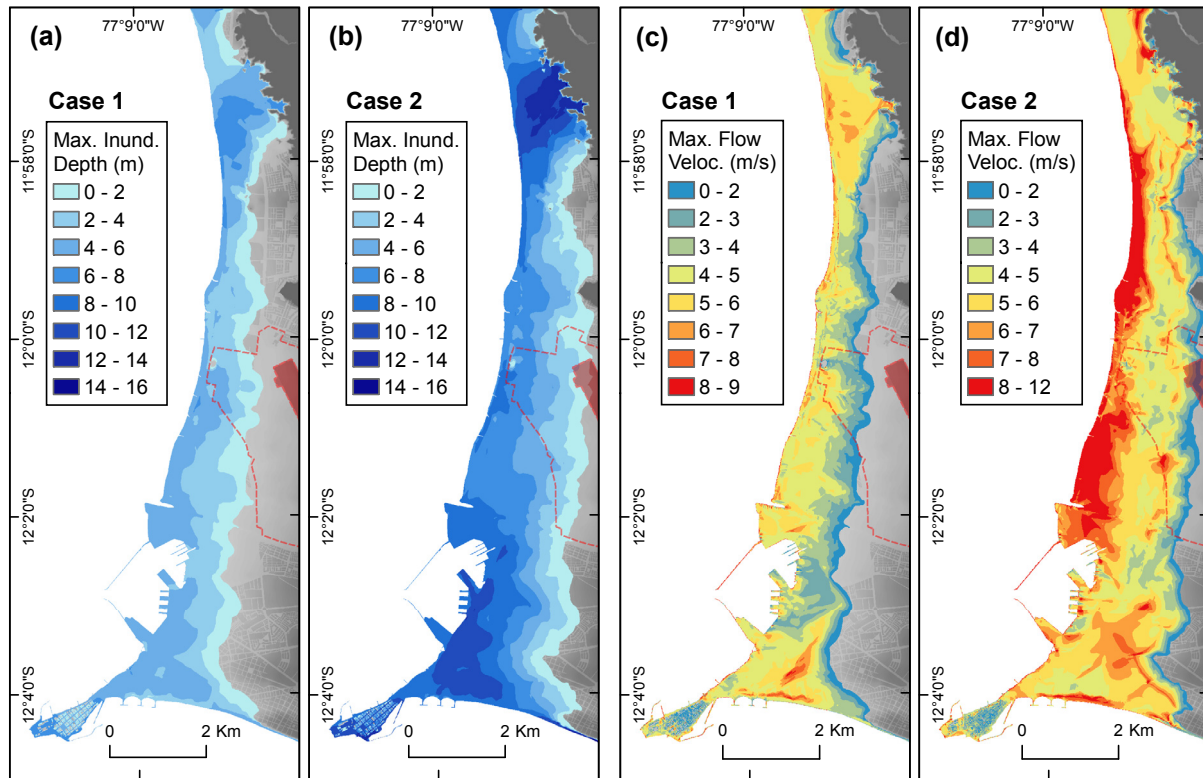
Fig. 3. Maximum tsunami inundation depth and flow velocity for the first ((a) and (c)) and the second ((b) and (d)) tsunami hazard scenario. (a) and (b) Maximum tsunami inundation depth. (c) and (d) Maximum tsunami flow velocity.

Table 2. Classification levels of building damage used in this study, categorized by MLIT. The illustrations were obtained and modified from [28].

Damage	Description	Condition	Illustration
Minor	No significant structural or non-structural damages	Possible to be use immediately	
Moderate	Slight damages to non-structural components	Possible to be use after moderate reparations	
Major	Significant damages to some walls but no damages in columns	Possible to be use after complete reparations and retrofitting	
Complete	Significant damages to several walls (more that half of wall density) and several columns	Possible to be use after major reparations	
Collapse	Destructive damage to walls and some columns	Lost of functionality. Non-repairable or great cost of retrofitting	
Whaled away	Washed away, only foundation remained, total overturned	Non-repairable, requires total reconstruction	
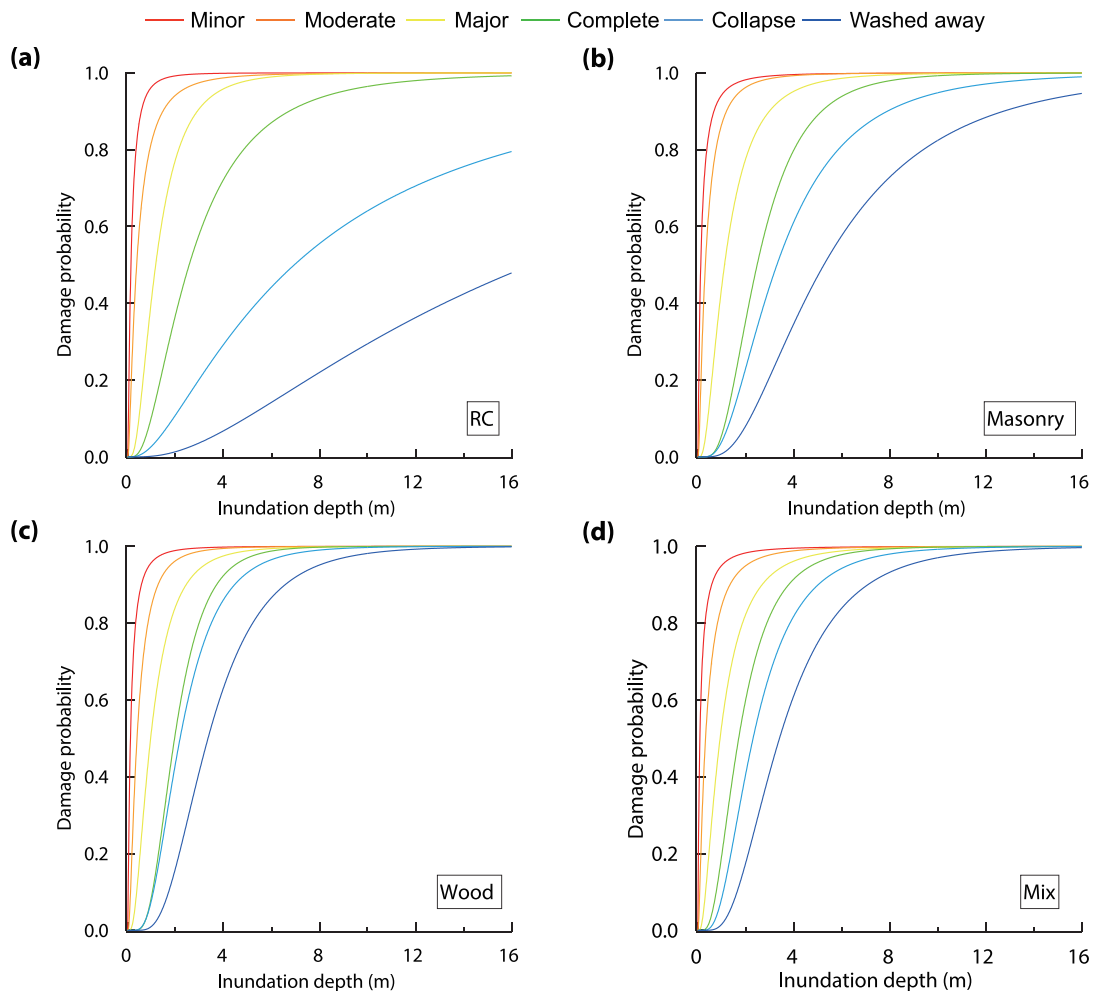
Fig. 4. Tsunami fragility curves based on structural material and damage levels. (a) RC, (b) masonry, (c) wood and (d) mixed-material buildings.

4.1. Application of Tsunami Fragility Functions

Tsunami fragility functions define the probability of structural damage due to tsunami inundation features, e.g., inundation depth and flow velocity, and are assumed to be cumulative probability P of damage occurrence (Eq. (1))

$$P(x) = \Phi \left[\frac{\ln x - \mu'}{\sigma'} \right] \quad \cdots \cdots \cdots \cdots \quad (1)$$

where Φ is lognormal distribution function, x is inundation depth, μ' and σ' are mean and standard deviation of $\ln x$. Statistic parameters of fragility function (μ' and σ') are obtained by plotting $\ln x$ and the inverse of Φ^{-1} in lognormal probability papers, and least-square-fitting this plot [29, 30].

Currently, several curves have been developed following major tsunami disasters for different site conditions. In the case of the Indian Ocean tsunami of 2004, for instance, fragility functions were developed for Banda Aceh, Indonesia [30], and Phang Nga, Thailand for RC buildings [31]. Following the 2010 Chilean tsunami in Dichato, Chile, for mixed material structures [32]. After the 2011 Tohoku tsunami with much more detail sur-

veyed data [33–35]. Considering the engineering features of building and site conditions, tsunami fragility functions are used to evaluate the damage probability of buildings using different tsunami hazard scenarios. Pioneering applications of tsunami fragility functions, in combination with numerical models, were presented at [36, 37]. These studies presented a preliminary straightforward-application of tsunami fragility for evaluating the damage probability of buildings within the inundated zone. Furthermore, Adriano et. al [38] extended and presented two different approaches for evaluating the probability of building damage using tsunami fragility curves.

In order to estimate the probability of building damage, we use tsunami fragility functions constructed by [34]. Suppasri et. al [34] used over 250,000 structures surveyed from Chiba to Aomori by the Ministry of Land, Infrastructure, Transport and Tourism (MLIT) of Japan. Specific curves were constructed based on the damage level, construction material, and number of stories. The six levels of damage to buildings adopted in [34], defined by the MLIT, are also used in this study. These levels and their descriptions are presented in **Table 2**. The probability of building damage is based on the four construction materials shown in **Table 1**. **Fig. 4** shows the set of

Table 3. Parameters for construction of tsunami fragility functions used in this study, according to [34].

	RC		Masonry		Wood		Others	
	μ'	σ'	μ'	σ'	μ'	σ'	μ'	σ'
Minor	-1.9636	1.0966	-2.1130	1.3362	-2.1216	1.2261	-2.4562	1.4874
Moderate	-0.9723	1.0600	-1.1573	1.0400	-0.9338	0.9144	-1.1373	1.1150
Major	0.1577	0.7090	0.1059	0.7693	-0.0400	0.7276	-0.0756	0.8277
Complete	0.9423	0.7522	0.9043	0.5746	0.6721	0.4985	0.5316	0.6235
Collapse	1.9381	1.0120	1.1918	0.6821	0.7825	0.5559	0.8336	0.6077
Washed away	2.8232	0.9635	1.6583	0.6913	1.2094	0.5247	1.2244	0.5723

fragility functions for different structural materials. These functions give a maximum classification of damage probability based on tsunami inundation depth. Note that RC structures have better performance than wood or masonry buildings. The parameter to construct the fragility curves are presented in **Table 3**.

4.2. Building Damage Estimation

We describe the methodology used to evaluate damage probability for buildings based on the damage level defined in **Table 2**. It is important to point out, however, that construction quality and building standards in central Peru are basically different from those in Japan, so the same load conditions may generate differences in building performance. Curves used in this study also include the contribution of ground shaking in the final damage stage. Nevertheless, considering the large database using in [34], recent fragility curves developed from the 2011 Tohoku event are the most appropriate to be applied in our study.

In a quantitative macroscale estimation of damage, the number of submerged buildings is first counted by using an analysis interval of 0.5 m for the inundation depth. Second, using a representative inundation value for each interval (mean value), the damage probability is estimated using respective fragility curves for individual construction material types. Third, the probable number of damage buildings in each interval for different construction materials is calculated by multiplying the number of submerged buildings by the probability damage or ratio of buildings damaged within the interval. Fourth, based on threshold values for building damage presented in [39], which are based on the material type and tsunami flow velocity acting on each structure, a realistic number of affected buildings is estimated for each damage level at each interval of inundation depth. Fifth, the probable damage level for each building structure and block-unit is assigned to the higher level of estimated damage for each structure.

4.3. Tsunami Vulnerability Mapping

Table 4 lists the total number and the percentage of probable affected buildings for the six modeled damage levels in each case scenario. The total number of submerged buildings are 1,753 and 2,114 for the Case 1 and the Case 2, respectively. In the Case 1, the percentage of washed away and survivor buildings are almost similar.

Table 4. Total number and percentage of probable damaged building for each damage level in the two hazard scenarios.

	Case 1		Case 2	
	# Build.	%	# Build.	%
Washed away	569	32.5	1315	62.2
Collapse	254	14.5	257	12.2
Complete	142	8.1	128	6.1
Major	124	7.1	63	3.0
Moderate	28	1.6	16	0.8
Minor	2	0.1	0	0.0
Survivor	634	36.2	335	15.8

In the Case 2 the percentage of washed away buildings ($> 60\%$) are significantly greater than the other damage levels. Comparing both cases, the percentage of washed away building is greater than the other damages levels.

Figure 5 shows the distribution of building damage for each hazard scenario. The extent of the inundation area is shown by the solid red line. Based on **Fig. 5**, buildings of the washed away level are largely concentrated in the central and northern sectors of the study area. **Fig. 6** shows the distribution of building damage in the La Punta district for each hazard scenario. Case 1 shows that the washed away state of damage probability is mostly concentrated in the surroundings of the district (**Fig. 6(a)**). In Case 2, washed away buildings are found throughout the whole district (**Fig. 6(b)**). An important point is regarding the designed evacuation building in this district, there are 19 buildings designed for vertical evacuation in case of tsunami [40], as shown by the white circle in **Fig. 6**. In Case 1, there are 3 buildings that present a washed away state of damage probability and 2 that present a complete or major state of damage probability. In Case 2, 6 buildings present a washed away state of damage probability and 2 present a collapsed and complete state of damage probability.

5. Conclusions

In this paper, we have presented an estimation of building damage for the Callao region of Peru based on tsunami fragility curves and tsunami numerical simulation. The damage level to buildings was estimated based on the construction material type. This study presents the first time that tsunami fragility curves were applied to the Callao
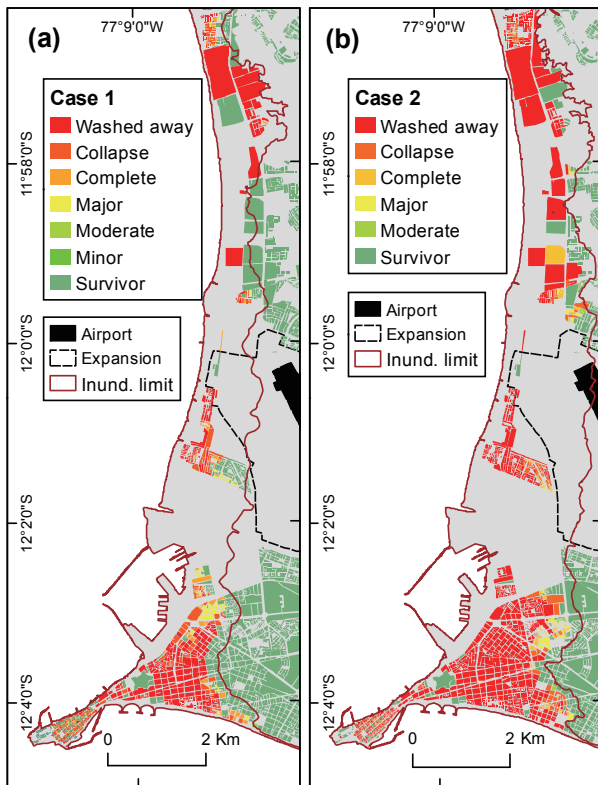
Fig. 5. Building damage assessment maps. (a) and (b) shows the probable damage level for the first and the second scenario. The solid solid red line shows the inundation limit of each scenario.

Fig. 6. Building damage level in the La Punta district. (a) and (b) shows the probable damage level for the first and the second scenario. White circles show the location of the designed evacuation building in the La Punta district.

region for estimating the damage level to structures. We used the six states of damage probability defined by the MLIT. Two tsunami hazard scenarios were assumed in assessing the damage probability of buildings. The first tsunami scenario represents the worse-case scenario of tsunami inundation that calculates the envelop of maximum inundation depth and flow velocity values from 12 probabilistic megathrust earthquake scenarios in central Peru. The second tsunami scenario corresponds to a historical tsunami event in this region. We provided a methodology for applying fragility curves for estimating building damage on a community scale.

Damage probability results show that in the case of the probabilistic hazard scenario, approximately 30% of all buildings in the inundation area may be washed away. In the case of the historical hazard scenario, however, over 60% of submerged buildings had a washed away state of damage probability.

Vulnerability maps are presented in this paper to support building damage assessment and land use planning in the study area.

References:

[1] S. L. Beck and L. J. Ruff, "Great earthquakes and subduction along the Peru trench," Physics of the Earth and Planetary Interiors, Vol.57, pp. 199-224, Nov. 1989.

[2] L. Dorbath, A. Cisternas, and C. Dorbath, "Assessment of the size of large and great historical earthquakes in Peru," Bulletin of the Seismological Society of America, Vol.80, No.3, pp. 551-576, 1990.

[3] C. Jimenez, N. Moggiano, E. Mas, B. Adriano, S. Koshimura, Y. Fujii, and H. Yanagisawa, "Seismic source of Callao 1746 earthquake obtained through tsunami numerical modeling," Journal of Disaster Research, Vol.8, No.2, p. 10, 2013.

[4] E. Mas, B. Adriano, H. Kuroiwa, and S. Koshimura, "Reconstruction process and social issues after the 1746 earthquake and tsunami in Peru: past and present challenges after tsunami events," in " Restoration and Reconstruction after Tsunami" (V. Santiago-Fandino, Y. Kontar, and Y. Kaneda (Eds.)), Springer, Netherlands, 2014 (in press).

[5] J. Kuroiwa, "Disaster reduction : living in harmony with nature," Lima: Editorial NSG S.A.C, first edited., 2004.

[6] Lima Aiport Partners, "Aeropuerto Internacional Jorge Chavez," 2013.

[7] N. Alam, M. S. Alam, and S. Tesfamariam, "Buildings' seismic vulnerability assessment methods: a comparative study," Natural Hazards, Vol.62, pp. 405-424, Jan. 2012.

[8] N. Pulido, H. Tavera, H. Perfettini, M. Chlieh, S. Aoi, S. Nakai, and F. Yamazaki, "Estimation of slip scenarios for magathrust earthquakes: A case of study for Peru," in 4th IASPEI / IAEE International Symposium, Effects of Surface Geology on Seismic Motion, University of California Santa Barbara, pp. 1-8, 2011.

[9] N. Pulido, H. Tavera, Z. Aguilar, M. Chlieh, D. Calderon, T. Sekiguchi, S. Nakai, and F. Yamazaki, "Mega-earthquakes rupture scenarios and strong motion simulations for Lima, Peru," in The International Symposium for CISMID 25th Anniversary, pp. 1-8, 2012.

[10] E. Mas, B. Adriano, N. Pulido, C. Jimenez, and S. Koshimura, "Simulation of tsunami inundation from future megathrust earthquake scenarios of Central Peru," Journal of Disaster Research, Vol.9, No.6, 2014.

[11] Instituto Nacional de Estadistica e Informatica (INEI; Institute of Statistic and Informatics), "Censos Nacionales 2007," 2007.

[12] D. Dominey-Howes, P. Dunbar, J. Varner, and M. Papathoma-Köhle, "Estimating probable maximum loss from a Cascadia tsunami," Natural Hazards, Vol.53, pp. 43-61, June, 2009.

[13] R. Omira, M. a. Baptista, J. M. Miranda, E. Toto, C. Catita, and J. Catalão, "Tsunami vulnerability assessment of Casablanca-Morocco using numerical modelling and GIS tools," Natural Hazards, Vol.54, pp. 75-95, Sept. 2009.

[14] G. R. Priest, C. Goldfinger, K. Wang, R. C. Witter, Y. Zhang, and A. M. Baptista, "Confidence levels for tsunami-inundation limits in northern Oregon inferred from a 10,000-year history of great earthquakes at the Cascadia subduction zone," Natural Hazards, Vol.54, pp. 27-73, Sept. 2009.

[15] A. Atillah, D. El Hadani, H. Moudni, O. Lesne, C. Renou, A. Mangin, and F. Rouffi, "Tsunami vulnerability and damage assessment in the coastal area of Rabat and Salé, Morocco," Natural Hazards and Earth System Science, Vol.11, pp. 3397-3414, Dec. 2011.

[16] D. M. Wiebe and D. T. Cox, "Application of fragility curves to estimate building damage and economic loss at a community scale: a case study of Seaside, Oregon," Natural Hazards, Vol.71, pp. 2043-2061, Dec. 2013.

[17] Centro de Estudios y Prevención de Desastres – PREDES, "Diseño de escenario sobre el impacto de un sismo de gran magnitud en Lima Metropolitana y Callo, Perú," tech. rep., Instituto Nacional de Defensa Civil - INDECI, Lima, Peru, 2009.

[18] PNUD/SDP-052/2009, "Investigación sobre el PELIGRO DE TSUNAMI en el Área Metropolitana de Lima y Callao," in SISTEMA DE INFORMACIÓN SOBRE RECURSOS PARA ATENCIÓN DE DESASTRES, COOPERAZIONE INTERNAZIONALE ? COOPI, 2010.

[19] B. Adriano, E. Mas, S. Koshimura, Y. Fujii, S. Yauri, C. Jimenez, and H. Yanagisawa, "Tsunami inundation mapping in Lima, for two tsunami source scenarios," Journal of Disaster Research, Vol.8, No.2, pp. 274-284, 2013.

[20] S. Koshimura, T. Katada, H. O. Mofjeld, and Y. Kawata, "A method for estimating casualties due to the tsunami inundation flow," Natural Hazards, Vol.39, pp. 265-274, Oct. 2006.

[21] A. Muhari, F. Imamura, S. Koshimura, and J. Post, "Examination of three practical run-up models for assessing tsunami impact on highly populated areas," Natural Hazards and Earth System Science, Vol.11, pp. 3107-3123, Dec. 2011.

[22] N. Mori, T. Takahashi, and The 2011 Tohoku Earthquake Tsunami Joint Survey Group, "Nationwide post event survey and analysis of the 2011 Tohoku Earthquake Tsunami," Coastal Engineering Journal, Vol.54, No.1, pp. 1250001-1, 2012.

[23] H. Gokon and S. Koshimura, "Mapping of Building Damage of the 2011 Tohoku Earthquake Tsunami in Miyagi Prefecture," Coastal Engineering Journal, Vol.54, No.1, pp. 1250006-1, 2012.

[24] A. Suppasri, S. Koshimura, K. Imai, E. Mas, H. Gokon, A. Muhari, and F. Imamura, "Damage Characteristic and Field Survey of the 2011 Great East Japan Tsunami in Miyagi Prefecture," Coastal Engineering Journal, Vol.54, No.1, pp. 1250005-1, 2012.

[25] A. Suppasri, N. Shuto, F. Imamura, S. Koshimura, E. Mas, and A. C. Yalciner, "Lessons Learned from the 2011 Great East Japan Tsunami: Performance of Tsunami Countermeasures, Coastal Buildings, and Tsunami Evacuation in Japan," Pure and Applied Geophysics, July 2012.

[26] M. Papathoma and D. Dominey-Howes, "Tsunami vulnerability assessment and its implications for coastal hazard analysis and disaster management planning, Gulf of Corinth, Greece," Natural Hazards and Earth System Science, Vol.3, No.6, pp. 733-747, 2003.

[27] F. Dall'Osso, M. Gonella, G. Gabbianelli, G. Withycombe, and D. Dominey-Howes, "A revised (PTVA) model for assessing the vulnerability of buildings to tsunami damage," Natural Hazards and Earth System Science, Vol.9, pp. 1557-1565, Sept. 2009.

[28] N. Leelawat, A. Suppasri, I. Charvet, and F. Imamura, "Building damage from the 2011 Great East Japan tsunami: quantitative assessment of influential factors," Natural Hazards, Feb. 2014.

[29] S. Koshimura, Y. Namegaya, and H. Yanagisawa, "Tsunami fragility: a new measure to identify tsunami damage," Journal of Disaster Research, Vol.4, No.6, pp. 479-488, 2009.

[30] S. Koshimura, T. Oie, H. Yanagisawa, and F. Imamura, "Developing fragility functions for tsunami damage estimation using numerical model and post-tsunami data from Banda Aceh, Indonesia," Coastal Engineering Journal, Vol.51, pp. 243-273, Sept. 2009.

[31] A. Suppasri, S. Koshimura, and F. Imamura, "Developing tsunami fragility curves based on the satellite remote sensing and the numerical modeling of the 2004 Indian Ocean tsunami in Thailand," Natural Hazards and Earth System Science, Vol.11, pp. 173-189, Jan. 2011.

[32] E. Mas, S. Koshimura, A. Suppasri, M. Matsuoka, M. Matsuyama, T. Yoshii, C. Jimenez, F. Yamazaki, and F. Imamura, "Developing Tsunami fragility curves using remote sensing and survey data of the 2010 Chilean Tsunami in Dichato," Natural Hazards and Earth System Science, Vol.12, pp. 2689-2697, Aug. 2012.

[33] A. Suppasri, E. Mas, S. Koshimura, K. Imai, K. Harada, and F. Imamura, "Developing tsunami fragility curves from the surveyed data of the 2011 great east Japan Tsunami in Sendai and Ishinomaki plains," Coastal Engineering Journal, Vol.54, No.1, pp. 1250008-1-1250008-1, 2012.

[34] A. Suppasri, E. Mas, I. Charvet, R. Gunasekera, K. Imai, Y. Fukutani, Y. Abe, and F. Imamura, "Building damage characteristics based on surveyed data and fragility curves of the 2011 Great East Japan tsunami," Natural Hazards, Vol.66, pp. 319-341, Nov. 2012.

[35] I. Charvet, I. Ioannou, T. Rossetto, A. Suppasri, and F. Imamura, "Empirical fragility assessment of buildings affected by the 2011 Great East Japan tsunami using improved statistical models," Natural Hazards, Mar. 2014.

[36] B. Adriano, E. Mas, S. Koshimura, and Y. Fujii, "Remote Sensing-based Assessment of Tsunami Vulnerability in the coastal area of Lima , Peru," in The 10th International Workshop on Remote Sensing for Disaster Management, Japan, pp. CD-ROM, 2012.

[37] B. Adriano, E. Mas, S. Koshimura, and Y. Fujii, "Tsunami Vulnerability Assessment of Buildings Using Remote Sensing Analysis and Numerical Modeling in Lima, Peru," in Proceedings of International Sessions in Coastal Engineering, JSCE, Vol.4, Vol.4, pp. CD-ROM, 2013.

[38] B. Adriano, E. Mas, and S. Koshimura, "Application of tsunami fragility functions for building damage assessment : two different approaches," in The APRU symposium series on Multi-hazards around the Pacific Rim, pp. CD-ROM, 2013.

[39] S. Hayashi, B. Adriano, E. Mas, and S. Koshimura, "Study of tsunami run-up model considering building failure," in Annual Meeting of the Tohoku Branch Technology Research Conference, Japan Society of Civil Engineers. Hachinohe, Japan., pp. CD-ROM, Tohoku University, 2014.

[40] E. Mas, B. Adriano, and S. Koshimura, "An Integrated Simulation of Tsunami Hazard and Human Evacuation in La Punta , Peru," Journal of Disaster Research, Vol.8, No.2, pp. 285-295, 2012.

Name:
Bruno Adriano

Affiliation:
Ph.D. Student, Graduate School of Engineering, Tohoku University

Address:
Aoba 468-1-E301, Aramaki, Aoba-ku, Sendai 980-0845, Japan
Brief Career:
2012-2013 Research student, ReGiD, IRIDeS, Tohoku University, Japan
2013- PhD Student, Graduate School of Engineering, Tohoku University
Selected Publications:
● B. Adriano, E. Mas, S. Koshimura, and Y. Fujii, "Tsunami Vulnerability Assessment of Buildings Using Remote Sensing Analysis and Numerical Modeling in Lima, Peru," in Proceedings of International Sessions in Coastal Engineering, JSCE, Vol.4, No.4, CD-ROM, 2013.
● B. Adriano, E. Mas, S. Koshimura, Y. Fujii, S. Yauri, C. Jimenez, and H. Yanagisawa, "Tsunami inundation mapping in Lima, for two tsunami source scenarios," J. of Disaster Research, Vol.8, No.2, pp. 274-284, 2013.
Academic Societies & Scientific Organizations:
● Japan Society of Civil Engineers (JSCE)
● Japan Geoscience Union (JpGU)
● Institute of Electrical and Electronics Engineers (IEEE)